Food and Bioprocess Technology (2026) 19:348
https://doi.org/10.1007/s11947-026-04418-7

RESEARCH

Concentration-Driven Structuring of Fresh Ginseng Starch Pastes: Linking Solid Loading to Fluid–Solid Transition, Mechanical Performance, and Swallowing Functionality

Jiyoon Kim[1,2,3] · Jung Soo Kim[1,2] · Kwang-Deog Moon[2] · Jung-Ho Lim[3] · Jeong-Seok Cho[3,4]

Received: 7 December 2025 / Accepted: 18 May 2026
© The Author(s), under exclusive licence to Springer Science+Business Media, LLC, part of Springer Nature 2026

Abstract
Fresh ginseng contains physiologically relevant bioactives but has limited application in texture-controlled systems due to its weak intrinsic network and processing-sensitive compounds. This study establishes a concentration-driven formulation framework in which ginseng starch powder functions as the primary structural variable governing physicochemical composition, antioxidant retention, rheological behavior, and deformation mechanics. Increasing powder concentration increased solids loading and promoted concentration-dependent network reinforcement, forming the structural basis for a controlled fluid–solid transition. Crude saponins and ginsenosides also increased with concentration, indicating improved retention within the denser paste matrix under the tested formulation conditions. Steady-shear and oscillatory tests showed reinforced shear-thinning behavior, greater elastic dominance, and enhanced dissipation capacity with increasing concentration. Tensile and compressive deformation results further demonstrated higher stiffness, reduced ductility, and intensified adhesion, reflecting network densification. IDDSI-based deformation tests supported these mechanical transitions under standardized low-stress loading, differentiating GP50 (Level 5), GP60 (Level 6), and GP70 (Level 7 easy-to-chew) textures. Sensory scores remained within a comparable perceptual range across formulations despite substantial differences in instrumental behavior. Multivariate analysis confirmed powder concentration as the dominant factor linking structural assembly to functional and sensory attributes. Overall, this concentration-driven strategy provides a formulation-level, structure–function-based and potentially scalable approach for designing soft-solid ginseng pastes tailored for dysphagia-oriented applications.

Keywords Solid loading · Soft-solid structuring · Fluid–solid transition · Rheology and mechanical properties · Ginseng starch paste · Dysphagia-friendly formulation

Introduction

Fresh ginseng (Panax ginseng C. A. Meyer) is widely recognized for its physiologically active constituents, including saponins and ginsenosides, which contribute to antioxidant, immunomodulatory, and anti-inflammatory functions (Lee et al., 2015; Sharma et al., 2023). These bioactivities highlight ginseng's potential as a functional ingredient for older adults and clinical populations experiencing oxidative stress and chronic inflammation (de Oliveira Zanuso et al., 2022). Despite this promise, the fibrous structure of ginseng tissues, heterogeneous particle distribution, and limited intrinsic gel-forming ability restrict its use in texture-controlled formulations. Furthermore, ginsenosides and related glycosides can degrade during heat and acid exposure (Zhao et al., 2019), complicating efforts to maintain both bioactivity and desirable structural performance during processing.

✉ Jeong-Seok Cho
jscho@kfri.re.kr

1 3D Food Printing Technology Research Institute, FOODPRO CO., Ltd., 14 Bokhyeon-Ro, Daegu 41530, Republic of Korea

2 School of Food Science and Biotechnology, Kyungpook National University, 80 Daehak-Ro, Daegu 41566, Republic of Korea

3 Smart Food Manufacturing Research Group, Korea Food Research Institute, Wanju-Gun 55365, South Korea

4 Department of Food Biotechnology, University of Science and Technology, Daejeon 34113, South Korea

Published online: 05 June 2026

Dysphagia management requires foods that flow predictably under low shear, deform cohesively under tongue–palate compression, and maintain bolus integrity during oral processing (Merino et al., 2020). Conventional approaches to designing such foods rely on multi-component systems incorporating potato, corn, or rice starches and hydrocolloids (Dick et al., 2021; Fiszman & Laguna, 2023; J. Kim et al., 2024a, 2024b). Although effective, these systems often involve multiple interacting variables, making it difficult to isolate mechanistic contributions of composition and processing. Consequently, rheology, structural reinforcement, and swallowing performance can become decoupled, posing challenges for process optimization and predictable behavior across batches.

For plant- and starch-based dispersions, solid loading, hydration patterns, and particle network development are known to dictate viscoelastic and mechanical properties. However, these process–structure–function relationships have not been mechanistically clarified in ginseng-based matrices (Zhuang et al., 2022). Rather than addressing this gap through molecular-level elucidation or starch-type comparative analyses, the present study approaches this issue from a formulation-level perspective, focusing on macroscopic structure–function behavior within a single starch system. Native ginseng starch exhibits fine granule size, moderate swelling, and stable viscosity (Koo et al., 2005a, 2005b), indicating its potential to act simultaneously as a structural scaffold and functional carrier. Yet, most prior ginseng food studies have focused on extracts, encapsulated compounds, or complex formulations (Pan et al., 2021), leaving a gap regarding simplified model systems in which formulation behavior can be systematically evaluated without introducing starch-type comparison or multi-component interactions.

Recent advances in soft-solid mechanics further suggest that solid concentration can strongly influence formulation-level crowding, network connectivity, and energy dissipation pathways in semi-solid matrices. In this context, powder concentration represents an engineering-relevant parameter capable of simultaneously modulating compositional enrichment and structural development (Costa et al., 2026). By using ginseng starch pastes as a single-starch model system within a fixed carrier matrix and without starch-type comparison or process-driven modifications, it becomes possible to evaluate how solid loading alone governs fluid-to-solid transitioning, nonlinear rheology, large-deformation behavior, and swallowability.

Importantly, the present study does not aim to prescribe texture thresholds for specific dysphagia subpopulations or to serve as a clinical swallowing assessment. Instead, it is designed as a formulation-level investigation that defines how solid loading governs mechanical transitions relevant to oral processing behavior. Such a framework is intended to function as a pre-formulation reference that can inform subsequent product-specific or clinically targeted optimization. Therefore, this study examines concentration-driven structuring in fresh ginseng starch pastes using a single-starch model system, by treating powder concentration as a single formulation control variable. By holding all other formulation parameters constant, this work establishes a formulation-level framework that links solid loading to fluid–solid transition behavior, mechanical performance, and IDDSI-classified swallowing functionality, without aiming to elucidate molecular-level mechanisms or comparative starch-type effects. Through integrated steady-shear and oscillatory rheology, tensile and compressive texture analysis, sensory evaluation, and multivariate statistics, this work proposes a structure–function-informed, formulation-focused strategy for creating texture-adapted, nutritionally enriched ginseng-based semi-solid foods intended for dysphagia-oriented applications. Within this framework, bioactivity-related composition was included not as an independent therapeutic endpoint, but to determine whether concentration-driven structuring could be achieved without compromising the functional value of the ginseng-based matrix. The findings further provide a formulation-level framework that can be extended to plant-based pastes in which solid loading is used as a primary driver of structural and functional performance.

Materials and Methods

Materials

Fresh ginseng (Panax ginseng C.A. Meyer, 6 years old) was purchased from a local market in Yeongju, Republic of Korea. Resistant maltodextrin, fructooligosaccharides syrup, and xanthan gum (food grade) were obtained from Samyang Corp. (Seoul, Republic of Korea). All chemicals used for compositional and antioxidant analyses were of analytical grade.

Extraction and Characterization of Native Ginseng Starch

Native starch was isolated following the method of Koo et al., (2005a, 2005b) with minor adjustments to improve yield and purity. Fresh ginseng roots were blended with distilled water (1:1, w/v) for 5 min, and the slurry was filtered through double-layered cheesecloth. The filtrate was centrifuged at 6000 × g for 10 min at 4 °C (Continent 512r, Hanil Science Industrial, Korea), and the resulting sediment was washed twice by resuspension in distilled water and recentrifugation. The repeated aqueous washing and sedimentation steps were designed to remove water-soluble proteins and low-molecular-weight components co-extracted during

Table 1 Formulation of ginseng starch pastes with different powder concentrations

Weight (g)					
Ginseng powder (GP)		Paste gel			
		Water	Nondigestiblemaltodextrin	Fructooligosaccharides	Xanthan gum
GP40	24				
GP50	30				
		29	15	15	1
GP60	36				
GP70	42				

GP40, GP50, GP60, and GP70 denote formulation codes indicating increasing ginseng powder levels across the concentration gradient

homogenization. Given the low solubility of starch granules under neutral aqueous conditions, residual protein content in the isolated starch fraction was considered minimal. The pellet was washed with 99% ethanol (2 × 500 mL), air-dried at 40 °C for 12 h, milled, and sieved through a 100-mesh screen. Starch was stored at − 20 °C until use. Moisture content and starch yield were determined according to AOAC (1984). The moisture content of fresh ginseng was 73.3 ± 2.4% (wet basis), and starch yield was 13.2 ± 4.8% (dry basis). Proximate composition analysis confirmed negligible protein content in the isolated starch fraction (Table S1), supporting its use as a starch-dominant model material.

Preparation of Ginseng Starch Paste Formulations

To prepare the carrier matrix, distilled water and fructooligosaccharides were homogenized at 14,900 rpm for 10 s (HR2535/00, Philips, Netherlands). Maltodextrin (Fibersol-2) and xanthan gum were progressively dispersed under homogenization for an additional 2 min. The mixture was heated to 85 °C for 30 min to ensure complete hydration, then cooled to ambient temperature. Extracted ginseng starch was subsequently incorporated into the pre-hydrated matrix according to the formulation ratios listed in Table 1. This sequence was intentionally selected to ensure homogeneous dispersion of starch particles within a stabilized viscous medium, thereby minimizing sedimentation or phase separation during equilibration. Importantly, starch gelatinization was not treated as a primary variable in this study. Instead, starch was introduced after matrix hydration to isolate the effect of powder concentration on macroscopic structure–function behavior under identical processing conditions. The resulting formulations generated a controlled concentration gradient spanning fluid-like dispersions, semi-solid systems, and soft-solid pastes. All samples were equilibrated at 4 ℃ for 24 h prior to testing to stabilize hydration and network development. The formulations were coded as GP40, GP50, GP60, and GP70 to indicate increasing ginseng powder levels across the concentration gradient. These sample names are formulation codes and do not represent exact percentages of ginseng powder based on the total paste weight.

Physicochemical Characterization

Moisture content was determined by AOAC (1984). Soluble solids were measured using a refractometer (Master-α, Atago, Japan) and recorded as °Brix. Color values (L^*, a^*, and b^*) were measured using a calibrated colorimeter (CR-400, Konica Minolta, Japan). These parameters were included to contextualize formulation effects on matrix hydration and compositional density.

Quantification of Total Sugars, Crude Saponins, and Ginsenosides

Total soluble sugars were measured using the phenol–sulfuric acid method (Dubois et al., 2002) with glucose as a standard. Crude saponins were quantified using the vanillin-sulfuric acid assay (Mursaliyeva et al., 2023). Ginsenoside profiling (Rg_1 and Rb_1) was performed using HPLC (LC-20A, Shimadzu, Japan) equipped with a C18 column (250 × 4.6 mm, 5 µm; Phenomenex, USA). A water–acetonitrile gradient was applied at 1 mL/min, and eluted compounds were detected by UV absorbance. These measurements provided compositional markers for evaluating concentration-dependent retention of bioactive functionality in the paste matrix.

Antioxidant Properties

Total phenolic content (TPC) was quantified using the Folin–Ciocalteu assay (J. S. Kim et al., 2024a, 2024b) and expressed as mg gallic acid equivalents (GAE) per 100 g of paste. Radical scavenging capacity was evaluated using DPPH (Brand-Williams et al., 1995) and ABTS (Ren et al., 1999) assays, and results were expressed as percentage inhibition relative to the control. These antioxidant indices were included to determine whether the concentration-driven structural changes in the starch matrix influenced the retention or degradation of ginseng-derived bioactive compounds.

Rheological Measurements for Fluid–Solid Transition Characterization

Rheological behavior was measured using a controlled-stress rheometer (HR-10, TA Instruments, USA) equipped

with a 20 mm parallel plate and a 1 mm gap at 25 ℃. Steady-shear apparent viscosity was recorded over a shear-rate range of 1–100 s^{-1}. Apparent viscosities at 10 and 50 s^{-1} were extracted from the viscosity curves to represent deformation conditions relevant to oral processing (Liu et al., 2023). Dynamic oscillatory tests were performed to characterize both linear and nonlinear viscoelasticity. After sample loading, the samples were allowed to rest for 3 min before measurement to minimize loading-induced structural disturbance and to ensure equilibration at 25 ℃. Frequency sweeps (0.01–100 rad s^{-1}) were conducted at 1% strain, which was selected within the linear viscoelastic region based on a prior strain-sweep test. The storage modulus (G'), loss modulus (G''), and complex viscosity (η^*) were recorded. Amplitude sweeps (0.01–100% strain, 1 Hz) were then performed to evaluate nonlinear viscoelastic behavior and to identify the strain corresponding to maximum viscous dissipation (G''max), which was used as the apparent yield criterion based on established nonlinear viscoelastic analysis (Hyun et al., 2011). Apparent yield stress (τ_γ) was subsequently estimated from $\tau = G^* \cdot \gamma$ at the strain corresponding to G''max. This analytical framework enabled evaluation of the concentration-dependent transition from flow-dominated to soft-solid behavior.

Tensile Deformation and Fracture Analysis

Tack-adhesion and tensile fracture behavior were analyzed using a texture analyzer (Compac-Ⅱ, Sunscientific, Japan) fitted with a 20 mm cylindrical probe. Samples (1.5 g) were equilibrated at 25 °C for 15 min, placed on the base plate, and stretched at 1 mm s^{-1} until rupture. The force–time curves were used to determine maximum tensile force (gf), rupture distance (mm), and optical fracture characteristics. Rupture distance was defined as the probe displacement at the point of sample fracture and was used as the primary indicator of extensibility/ductility under tensile loading.

Texture Profile Analysis (TPA)

TPA was performed using the same texture analyzer equipped with a 25 mm cylindrical probe. Samples were compressed twice to 50% height at 1 mm s^{-1}, and hardness, cohesiveness, adhesiveness, and springiness were calculated from the force–time curves. Ten replicates were conducted. These parameters were used to evaluate concentration-dependent changes in structural reinforcement and to interpret how the pastes progressed from deformable fluid-like gels to cohesive, soft-solid matrices.

IDDSI Level Classification

Swallowability assessment followed the International Dysphagia Diet Standardisation Initiative (IDDSI, 2019). For each sample, 15 g of paste was evaluated using spoon tilt, fork drip, and fork pressure tests to classify IDDSI Levels 5–7, corresponding to Minced & Moist, Soft & Bite-Sized, and Easy to Chew, respectively. Spoon-tilt testing assessed geometric retention and cohesive sliding; fork drip evaluated flowability through tines. Fork-pressure resistance was interpreted relative to the approximate 17 kPa tongue-pressure benchmark (Steele et al., 2015). IDDSI outcomes were compared with rheological and TPA results to contextualize how concentration-driven structural transitions altered the paste's deformation behavior under simulated oral conditions.

Sensory Evaluation

Sensory evaluation was conducted to capture perceptual descriptors associated with oral processing behavior under controlled conditions, rather than to perform clinical swallowing assessment. Thirty trained panelists (15 males and 15 females; aged 25–35) from Kyungpook National University participated after completing two training sessions focused on attribute definition and scale calibration. Samples (20 g) were served at room temperature under controlled lighting conditions, with palate cleansing between samples. Three attributes were evaluated using a 10-point structured scale: ease of oral transport (0 = very difficult; 10 = very easy), ease of palatal release (0 = highly adhesive; 10 = non-adhesive), and overall acceptability (0 = very low; 10 = very high). Sensory measurements were used to examine perceptual responses related to oral transport and oral adhesion behavior across formulations. The study protocol was approved by the Institutional Review Board of Kyungpook National University (KNU-2023–486) and conducted in accordance with the Declaration of Helsinki.

Integrated Correlation and Multivariate Analysis

To investigate structural–functional coupling, Pearson's correlation analysis was conducted using triplicate means. Instrumental color parameters (L^*, a^*, and b^*) were excluded, as they served as quality indicators rather than structural variables. Principal component analysis (PCA) was performed after z-score normalization as a descriptive multivariate tool to examine whether independently measured compositional, rheological, mechanical, and sensory variables aligned coherently along the imposed concentration gradient, rather than to derive predictive or causal relationships. Analyses were conducted in Python v3.14 using pandas, scikit-learn, scipy, and matplotlib, and seaborn was used for heatmap visualization.

Table 2 Physicochemical characteristics and antioxidant capacities of ginseng starch pastes with different powder concentrations

	Physicochemical characteristics					Antioxidant capacitiesAQ		
	Moisture content (%)	Soluble solids (°Brix)	Color values			Total phenol content (mg TAE/kg)	DPPH radical scavenging activity (%)	ABTS radical scavenging activity (%)
			L*	a*	b*			
GP40	39.0 ± 0.2a	5.0 ± 0.0a	58.0 ± 0.4a	4.2 ± 0.2b	28.4 ± 0.5c	842.7 ± 21.7c	2.0 ± 0.1d	2.4 ± 0.1d
GP50	37.7 ± 0.3b	5.2 ± 0.0a	55.4 ± 0.6b	4.8 ± 0.4a	29.5 ± 0.2a	882.1 ± 8.2c	2.3 ± 0.1c	2.9 ± 0.1c
GP60	34.8 ± 0.1c	5.1 ± 0.0a	55.9 ± 0.5b	4.9 ± 0.2a	28.8 ± 0.4b	956.5 ± 10.9b	3.1 ± 0.1b	3.8 ± 0.1b
GP70	33.8 ± 0.3d	5.2 ± 0.0a	55.4 ± 0.3b	5.1 ± 0.2a	28.9 ± 0.1b	1042.5 ± 35.8a	3.8 ± 0.1a	5.0 ± 0.1a

GP40, GP50, GP60, and GP70 denote formulation codes indicating increasing ginseng powder levels across the concentration gradient. Values are expressed as mean ± standard deviation ($n = 3$, color values; $n = 5$). Different superscript letters (a–d) indicate significant differences among sample groups according to Duncan's multiple range test ($p < 0.05$)

Statistical Analysis

All experiments were performed in triplicate unless otherwise noted. One-way ANOVA with Tukey's post hoc test ($p < 0.05$) was used to evaluate differences among formulations. Pearson's correlations quantified relationships among compositional, structural, and sensory variables.

Results and Discussion

Physicochemical Characteristics and Concentration-Dependent Compositional Patterns

The physicochemical properties of ginseng starch pastes prepared at different powder concentrations are summarized in Table 2. Moisture content was highest in GP40 (39.0 ± 0.2%) and decreased progressively with increasing solid loading. This trend is consistent with increasing solid content and effective crowding in the matrix, which accompanied the development of more cohesive and deformation-resistant structures under the present formulation conditions. Soluble-solid content remained statistically unchanged across formulations. This pattern may be attributable to the limited solubility of the added ginseng powder, which likely contributed predominantly to the insoluble fraction rather than to the dissolved fraction measured by refractometry. Color parameters showed a consistent concentration dependence: lightness (L^*) decreased while redness (a^*) and yellowness (b^*) increased as powder concentration increased. These chromatic shifts correspond to the higher pigment density associated with greater ginseng solid incorporation and are consistent with the optical behavior of concentrated ginseng matrices reported in freeze-dried systems (Xiang et al., 2024). Although color is not a structural variable and does not directly reflect bulk microstructure, the concentration-dependent chromatic shifts indicate formulation-level consistency in ginseng solid incorporation across samples prepared under identical mixing and equilibration conditions. In this context, surface color parameters are interpreted as a qualitative indicator of concentration tracking rather than as direct evidence of bulk dispersion or microstructural uniformity.

The physicochemical features of the native ginseng starch used in this study—moderate amylose content (~ 34%), limited swelling power, and narrow granule size distribution (Koo et al., 2005a, 2005b)—provide a structural basis for the cohesive, weak-gel-like networks observed throughout the concentration gradient. Overall, increasing powder concentration systematically decreased moisture, intensified chromatic density, and preserved soluble-solids uniformity. These compositional conditions define the baseline from which the concentration-driven fluid–solid transition behaviors described in subsequent sections emerge.

Functional Composition and Antioxidant Retention in a Concentration-Dependent Ginseng Starch Matrix

The functional components of the ginseng starch pastes, including total sugars, crude saponins, ginsenosides, and antioxidant capacities, exhibited clear concentration-dependent trends (Table 2, Fig. 1). Total sugar content was highest in GP40 (960.4 mg mL^{-1}) and decreased with increasing powder concentration. This trend may reflect a combination of formulation-level compositional displacement and methodological factors associated with sugar extraction and quantification in highly concentrated starch matrices. As powder concentration increased, the relative proportion of insoluble starch granules increased while soluble carbohydrate components, including resistant maltodextrin and fructooligosaccharides added at fixed levels, constituted a smaller fraction of the total matrix.

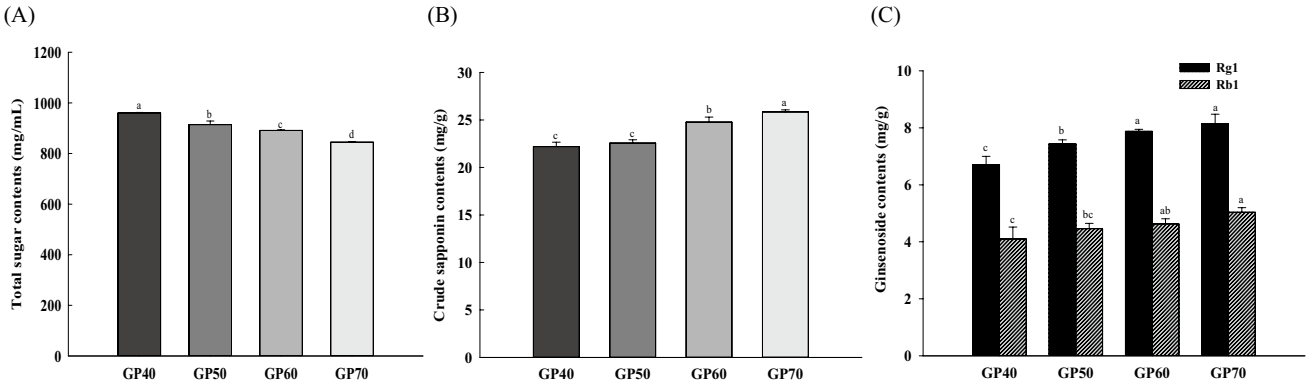


Fig. 1 Concentration-dependent changes in functional components and antioxidant capacities indicating matrix-mediated biochemical retention. GP40, GP50, GP60, and GP70 denote formulation codes indicating increasing ginseng powder levels across the concentration gradient. Values are expressed as mean ± standard deviation ($n = 5$). Different superscript letters (a–d) indicate significant differences among sample groups according to Duncan's multiple range test ($p < 0.05$)

In addition, increased solid crowding at higher concentrations may limit extraction efficiency or assay accessibility for soluble sugars, potentially contributing to an apparent decrease in measured total sugar content. Similar analytical constraints have been reported in concentrated carbohydrate systems, where particle-dominated matrices reduce the effective recoverable soluble fraction (Oberoi & Sogi, 2015). Accordingly, the observed decline in total sugar content is interpreted as a formulation-level trend reflecting increased solid dominance rather than as a definitive measure of absolute compositional loss.

Crude saponins and the representative ginsenosides Rg1 and Rb1 increased proportionally with powder concentration, reaching 25.9 mg g^{-1}, 8.2 mg g^{-1}, and 5.0 mg g^{-1}, respectively, in GP70. These values correspond to approximately 60–70% retention relative to the native powder, aligning with the stability typically observed under minimal thermal and acidic stress (Cho et al., 2014; Sharma et al., 2023). The monotonic increase across formulations suggests that structurally denser matrices may provide a more protective matrix environment during paste formation. Importantly, the observed stabilization is interpreted at the formulation level and not as evidence of specific molecular interactions or binding between ginsenosides and starch chains. Within the scope of the present study, no attempt was made to resolve hydrogen bonding specificity, hydrophobic interactions, or complex formation at the molecular scale. Instead, the results indicate that native ginseng starch pastes can provide a sufficiently dense matrix environment to support retention of bioactive components during processing. Comparable stabilization trends associated with matrix densification and restricted mass transfer have been reported in starch-polyphenol and carbohydrate-phytochemical systems (Cui et al., 2024), supporting the formulation-level interpretation adopted here.

Antioxidant properties measured via TPC, DPPH, and ABTS assays also increased with solid loading. TPC rose from 842.7 ± 21.7 mg TAE kg^{-1} (GP40) to 1042.5 ± 35.8 mg TAE kg^{-1} (GP70), while DPPH and ABTS scavenging activities nearly doubled over the same concentration range. These trends parallel the increased retention of saponins and ginsenosides and further support the interpretation that denser matrix organization may contribute to improved retention. The enhanced antioxidant capacity cannot be explained solely by higher solid mass; instead, it may reflect matrix-associated retention within the hydrated starch-rich network, which reduces exposure to oxygen and reactive species. Similar protective interactions have been documented for gelatinized starch systems forming weak complexes with polyphenolic molecules, thereby enhancing radical-scavenging performance (Bu et al., 2023; Liu et al., 2020).

From a formulation-level process–structure–function perspective, these results indicate that powder concentration influences both compositional enrichment and the retention of ginseng-derived functional components. Increasing solid loading increased the density of bioactive compounds and was associated with improved retention under the denser matrix conditions examined in this study. Within the scope of the present work, these concentration-dependent trends provide a supportive functional context for evaluating how structural transitions are related to rheological behavior, mechanical deformation, and swallowing-related performance in the subsequent sections.

Rheological Behavior and Concentration-Dependent Modulation of Flow, Viscoelasticity, and Swallowing-Related Mechanical Performance

The rheological profiles of the ginseng starch pastes showed a clear concentration-dependent modulation of flow and

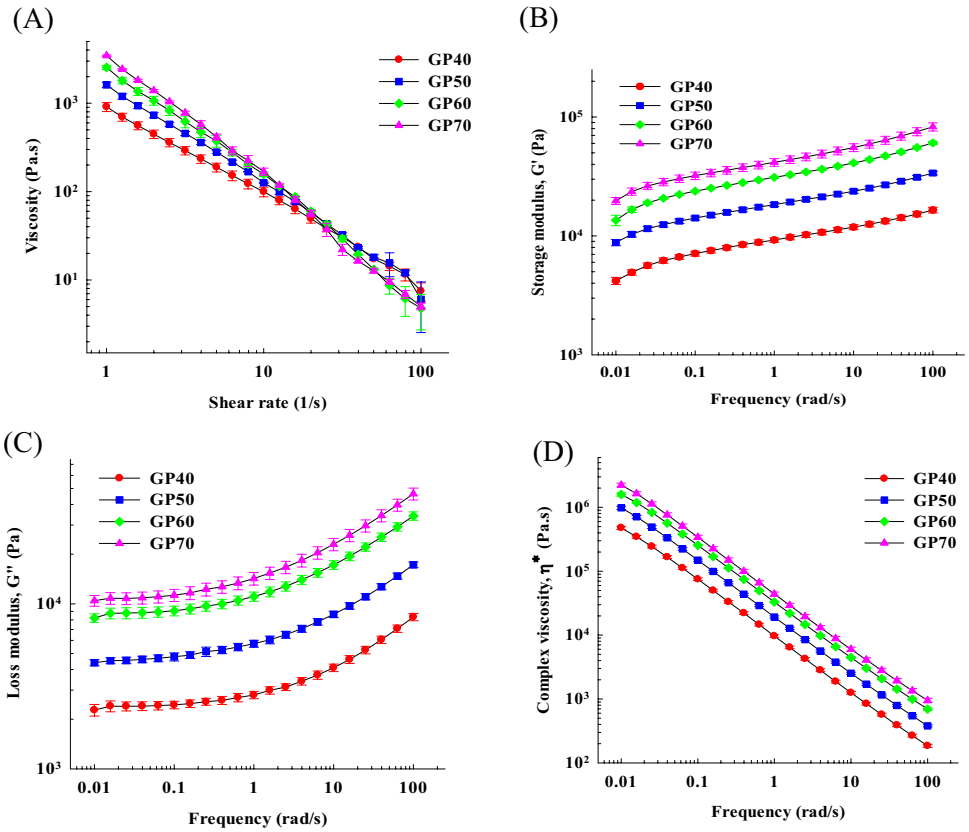


Fig. 2 Steady-shear and oscillatory rheology illustrating the concentration-governed fluid–solid transition. GP40, GP50, GP60, and GP70 denote formulation codes indicating increasing ginseng powder levels across the concentration gradient. Mean values ($n = 10$)

viscoelastic behavior (Fig. 2; Table 3). All samples exhibited pronounced shear-thinning behavior over the shear-rate range of 1–100 s^{-1}, confirming their non-Newtonian character. Apparent viscosity at 10 s^{-1} (η_{10}) increased progressively from GP40 to GP70, indicating greater low-shear flow resistance as powder concentration increased (Singh & Kaur, 2017). In contrast, apparent viscosity at 50 s^{-1} (η_{50}) decreased markedly in all formulations, and the

Table 3 Steady-shear, oscillatory, and non-linear rheological parameters of ginseng starch pastes with different powder concentrations

Parameter	GP40	GP50	GP60	GP70
Steady-shear rheology				
η_{10}	99.9 ± 12.5^{c}	126.1 ± 2.2^{b}	157.6 ± 8.8^{a}	168.7 ± 15.6^{a}
η_{50}	17.3 ± 0.6^{a}	17.0 ± 0.8^{a}	13.2 ± 0.4^{b}	12.6 ± 0.7^{b}
Oscillatory rheology				
G' at 100% strain (kPa)	16.53	33.80	60.63	82.80
G'' at 100% strain (kPa)	8.33	17.24	34.08	46.41
Complex modulus G^* ($\gamma = 100\%$) (kPa)	18.47	37.95	69.46	94.66
Non-linear rheology				
Apparent yield stress (τ_γ) (kPa)	18.47	37.95	69.46	94.66
Yield strain criterion	G''max	G''max	G''max	G''max
G'–G'' crossover within 0.01–100% strain	No	No	No	No

GP40, GP50, GP60, and GP70 denote formulation codes indicating increasing ginseng powder levels across the concentration gradient. Steady-shear apparent viscosities at 10 and 50 s^{-1} (η_{10} and η_{50}) were extracted from viscosity curves measured over 1–100 s^{-1} and are reported as mean values. Oscillatory and non-linear rheological parameters were obtained from amplitude sweeps conducted at 1 Hz over 0.01–100% strain after a 3-min equilibration period following sample loading. Apparent yield stress (τ_γ) was determined at the strain corresponding to the maximum loss modulus (G''max), because no G'–G'' crossover was observed within the tested strain range. Values are presented as mean values, and oscillatory/non-linear parameters were reported without statistical comparison

concentration-dependent separation observed at low shear became substantially reduced at higher shear rates. This pattern suggests that the more concentrated systems were more shear sensitive under elevated shear conditions, consistent with greater flow-induced structural disruption (Stading, 2021).

Dynamic oscillatory measurements further showed that G' remained higher than G'' across the measured frequency range, indicating weak-gel-like viscoelastic behavior in all formulations. Both moduli increased with powder concentration, demonstrating progressively greater elastic resistance and structural reinforcement in the more concentrated pastes (Guan et al., 2024). Complex viscosity (η^*) decreased with increasing frequency, consistent with frequency-dependent structural relaxation in semi-solid viscoelastic systems. These results collectively indicate that increased solids loading shifted the system toward a more elastic and more deformation-resistant state at the macroscopic level (Li et al., 2023).

Amplitude sweep analysis provided additional insight into non-linear deformation behavior. No G'–G'' crossover was observed up to 100% strain in any formulation, indicating that classical crossover-defined yielding did not occur within the tested range. Therefore, the strain corresponding to the maximum loss modulus (G''max) was used as the apparent yield criterion, following established LAOS-based interpretation. Based on this criterion, apparent yield stress (τ_γ) increased sharply from 18.47 kPa in GP40 to 94.66 kPa in GP70, representing a more than fivefold increase in resistance to large-deformation breakdown. This trend supports the interpretation that increasing powder concentration progressively strengthened the macroscopic resistance of the paste matrix to imposed strain. In formulation terms, the decrease in η_{50} across the concentration range indicates that all samples remained shear-responsive under elevated deformation, whereas the marked increase in apparent yield stress from GP40 to GP70 reflects progressively greater resistance to structural breakdown. When considered together with the IDDSI outcomes, these rheological shifts support the transition from more easily deformable pastes (GP50, Level 5) toward increasingly deformation-resistant soft solids (GP60, Level 6; GP70, Level 7).

It should also be noted that ginseng starch was incorporated after thermal preparation of the carrier matrix. Accordingly, classical heat-induced starch gelatinization was not treated as an independently controlled variable in this system. Although post-addition hydration and swelling of starch granules during equilibration may have contributed to the measured rheological responses, these effects were intrinsically coupled to powder concentration under identical processing conditions. Accordingly, the concentration-dependent rheological reinforcement is interpreted here at the formulation level as reflecting increased solids loading and denser matrix development, rather than direct evidence of a specific microscopic mechanism. Overall, increasing powder concentration shifted the ginseng starch pastes from more flow-dominant dispersions toward more elastic and deformation-resistant soft-solid systems. In this study, powder concentration is therefore interpreted as a formulation-level control variable that integrates concurrent changes in solids loading, hydration, and macroscopic structural development, rather than as a single mechanistic determinant.

Mechanical Deformation Behavior and Texture Profile Characteristics Relevant to Swallowing Performance

Tensile Deformation and Fracture Behavior

Tensile deformation analysis (Fig. 3) revealed distinct concentration-dependent transitions in the extensional mechanics of ginseng starch pastes. Maximum tensile force increased markedly from GP40 to GP70, indicating that greater solid loading enhanced resistance to applied tensile stress through strengthened granular-polymeric connectivity. In this system, starch hydration and structural contribution are better considered as a concentration-governed continuum rather than as discrete fractions of ungelatinized and fully gelatinized starch. Such behavior is consistent with soft-matter systems in which particle crowding and closer matrix association promote tighter network entanglement and stronger probe–matrix interactions (Gibouin et al., 2022; Methacanon et al., 2023). Conversely, rupture distance decreased significantly with increasing concentration, and high-solid formulations exhibited sharper, brittle-like fracture surfaces. This behavior indicates reduced deformation capacity prior to failure and reflects increasing structural restriction under tensile loading. As solid loading increases, the matrix becomes less capable of large-scale rearrangement, leading to earlier fracture under extensional stress, characteristics commonly observed in concentrated starch or hydrocolloid systems (Nishinari et al., 2019). These patterns parallel the increased elastic dominance observed in oscillatory rheology (Sect. "Rheological Behavior and Concentration-Dependent Modulation of Flow, Viscoelasticity, and Swallowing-Related Mechanical Performance"), demonstrating that starch concentration governs structural consolidation across both shear- and extension-based deformation pathways.

Texture Profile Characteristics

Compression-based texture profile analysis (Table 4) further illustrated the mechanical evolution induced by concentration. Hardness and gumminess increased substantially from GP40 to GP70, reflecting progressive

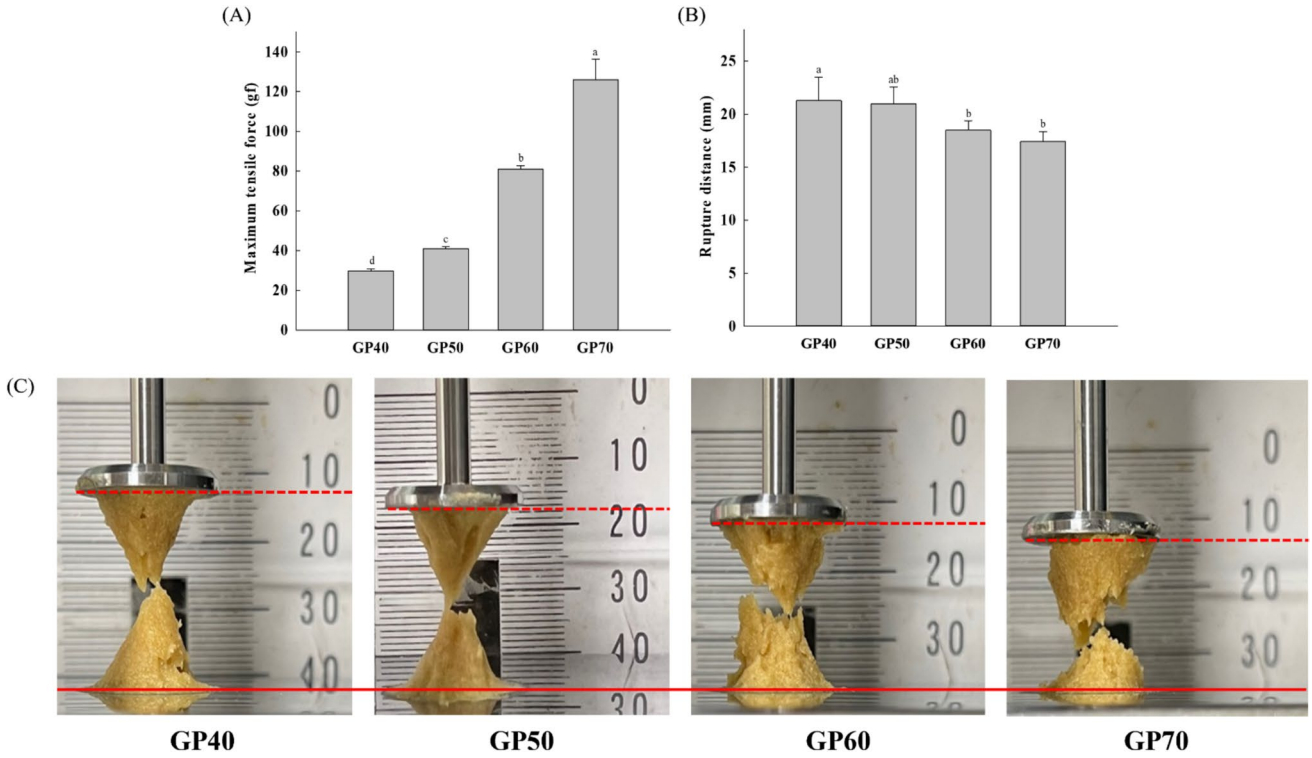


Fig. 3 Tensile deformation and fracture behavior of ginseng starch pastes at different powder concentrations. GP40, GP50, GP60, and GP70 denote formulation codes corresponding to increasing ginseng powder levels. Values are expressed as mean ± standard deviation ($n = 10$). Different superscript letters (a–d) indicate significant differences among sample groups according to Duncan's multiple range test ($p < 0.05$). The solid line indicates the initial reference position, while the dashed line represents the fracture point. Rupture distance was defined as the probe displacement between these two positions

Table 4 Texture profile analysis of ginseng starch pastes with different powder concentrations

Samples	Hardness (gf/cm^2)	Cohesiveness (%)	Adhesiveness (gf)	Gumminess (%)
GP40	161.1 ± 40.4^{c}	123.3 ± 18.9^{a}	−83.4 ± 22.0^{a}	287.2 ± 44.2^{c}
GP50	278.2 ± 85.9^{c}	118.8 ± 13.7^{ab}	−154.0 ± 49.4^{a}	465.5 ± 108.5^{c}
GP60	511.4 ± 61.8^{b}	111.4 ± 5.9^{ab}	−254.3 ± 33.5^{b}	837.3 ± 150.0^{b}
GP70	1129.9 ± 200.8^{a}	97.5 ± 1.4^{b}	−543.3 ± 79.8^{c}	1606.0 ± 294.7^{a}

GP40, GP50, GP60, and GP70 denote formulation codes indicating increasing ginseng powder levels across the concentration gradient. Values are expressed as mean ± standard deviation ($n = 5$). Different superscript letters (a–c) indicate significant differences among sample groups according to Duncan's multiple range test ($p < 0.05$)

reinforcement of the semi-solid matrix and reduced ability of the network to dissipate energy under compressive strain. Cohesiveness decreased with concentration, indicating reduced internal continuity as solid–solid contacts dominate and the capacity for structural recovery diminishes (Rahman & Al-Farsi, 2005). This trend was also in line with the reduced ductility and more brittle fracture behavior observed in the tensile test, suggesting progressively greater fragility as powder concentration increased. Adhesiveness increased significantly at higher concentrations, likely due to stronger surface interactions and reduced surface lubrication under the more concentrated conditions (Lee & Rhee, 2007). These compressive trends align with the increased low-shear viscosity (η_{10}) and the marked rise in apparent yield stress (τ_γ), indicating progressive structural reinforcement with increasing solid loading (Guan et al., 2024; Witt & Stokes, 2015). Importantly for food-processing applications, this stiffening trajectory implies that formulation adjustments based solely on powder concentration can be used to tune handling behavior, depositional stability, and deformation resistance during portioning or packaging.

Implications for Swallowing Safety and Oral Transport Efficiency

Integrating tensile, compressive, and viscoelastic results provides a quantitative basis for understanding how concentration modulates oral-processing mechanics. Lower-concentration samples (GP40–GP50), characterized by greater ductility and moderate compressive resistance, are more capable of forming cohesive boluses under tongue–palate compression thresholds (~ 17 kPa), aligning with mechanical conditions recommended for dysphagia-oriented foods (Steele et al., 2015). Intermediate concentrations (GP50–GP60) achieved a balance between deformation resistance and matrix integrity, supporting controlled oral transport while maintaining adequate flow response under IDDSI-style compressive loading. In contrast, GP70 exhibited markedly higher hardness, reduced cohesiveness, and brittle fracture behavior—mechanical traits that increase structural stability during handling but may exceed the deformation tolerance of individuals with impaired swallowing efficiency (Merino et al., 2020). From an engineering standpoint, these results confirm that powder concentration serves as a single, effective structural variable that modulates both manufacturability (portioning, shaping, and handling) and oral-processing performance. Together, these findings demonstrate that powder concentration governs both manufacturability-related deformation mechanics and in-mouth transport behavior through a shared structural mechanism, reflecting a coherent process–structure–function relationship characteristic of semi-solid food systems.

IDDSI-Based Swallowability Validation of Concentration-Modulated Ginseng Starch Pastes

To determine how the concentration-dependent mechanical transitions described in Sect. "Mechanical Deformation Behavior and Texture Profile Characteristics Relevant to Swallowing Performance" translated to practical deformation performance, the ginseng starch pastes were evaluated using the International Dysphagia Diet Standardisation Initiative (IDDSI) testing protocol. Although originally developed for clinical assessment, IDDSI tests operate as quasi-static deformation procedures that approximate confined compression, cohesive sliding, and shape retention under low-stress loading (Steele et al., 2015). As such, they provide a complementary engineering-based validation of soft-solid mechanics and bolus deformability in semi-solid food matrices.

In the spoon-tilt test, GP40 displayed strong surface adhesion and insufficient structural release, consistent with its high cohesiveness and ductile fracture behavior (Table 5). These characteristics prevented compliance with Level 5 criteria, as excessive surface tackiness limited controlled sliding (Yu et al., 2023). GP50, however, maintained geometric stability while detaching cleanly from the spoon, meeting Level 5 specifications. Fork-pressure testing confirmed that GP50 deformed fully under minimal force, remaining below the approximate 17 kPa threshold commonly associated with tongue–palate compression (Steele et al., 2015).

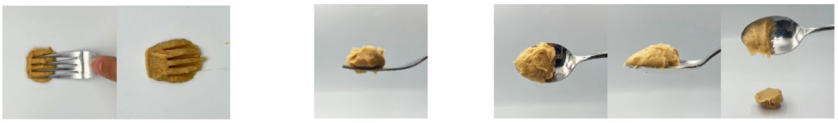
With increased concentration, the pastes exhibited more elastic resistance and partial shape retention. GP60 qualified as Level 6, undergoing smooth deformation without structural collapse, indicative of a moderately elastic soft solid (Bitencourt et al., 2023). GP70, the most concentrated formulation, fractured cleanly under fork pressure without crumbling and met Level 7 easy-to-chew requirements (Kim et al., 2025). These behaviors correspond well with the increased hardness, reduced ductility, and brittle fracture patterns observed in mechanical tests (Sect. "Mechanical Deformation Behavior and Texture Profile Characteristics Relevant to Swallowing Performance") and reflect the denser networks described in concentrated biopolymer systems (Nishinari et al., 2019).

Overall, IDDSI outcomes showed strong agreement with shear rheology and large-deformation mechanics, confirming that powder concentration functions as a primary structural parameter governing the transition from cohesive, ductile pastes to rigid, shape-retaining soft solids. The alignment across independent deformation modes demonstrates that concentration-driven modulation enables predictable structural performance under standardized low-stress loading. From a methodological perspective, the IDDSI framework is inherently threshold-based rather than continuous, classifying materials according to discrete deformation and shape-retention criteria rather than enabling regression-based prediction. Accordingly, the present analysis emphasizes formulation-level mapping between concentration, mechanical response, and IDDSI classification, rather than quantitative predictive modeling.

Importantly, these concentration-dependent transitions are consistent with behaviors previously reported for potato- and corn-starch-based dysphagia-oriented systems (Dick et al., 2021; Fiszman & Laguna, 2023), indicating that the observed responses primarily reflect a general starch behavior governed by solid loading rather than starch-type-specific phenomena. Accordingly, the absence of direct starch-type control groups represents an intentional formulation design choice aimed at isolating powder concentration as the dominant structural variable while minimizing confounding effects associated with differences in starch morphology or hydration kinetics. By adopting a single-starch model system, the present study establishes a concentration-driven formulation framework applicable to semi-solid starch-based matrices, rather than demonstrating material-specific functional advantages of ginseng starch.

Although GP70 met IDDSI Level 7 criteria, its markedly increased hardness and reduced ductility indicate that such

Table 5. Classification of ginseng starch pastes based on the IDDSI (International Dysphagia Diet Standardisation Initiative) framework tests

Sample	IDDSI TEST			
	Fork pressure test	Fork drip test	Spoon tilt test	Level
GP40				Not classified
GP50				Level 5 (Minced & moist)
	Fork pressure test		Spoon pressure test	Level
GP60				Level 6 (Soft & Bite-sized)
	Fork pressure test	Spoon pressure test	Cut or break apart	Level
GP70				Level 7 (Easy to chew)

GP40, GP50, GP60, and GP70 denote formulation codes indicating increasing ginseng powder levels across the concentration gradient.

high solid loadings may exceed the safe deformation tolerance for individuals with impaired swallowing function. From a dysphagia management perspective, formulations at this concentration may pose increased risks related to bolus fragmentation or esophageal obstruction, particularly in populations with reduced tongue–palate strength or delayed swallow initiation. Accordingly, GP70 is discussed as an upper-bound structural reference defining the limits of concentration-driven reinforcement, rather than as a recommended formulation for dysphagia-oriented applications. The combined rheological and IDDSI results indicated that increasing solids loading was associated with a progressive shift from more easily deformable pastes toward more deformation-resistant soft-solid structures across the observed Levels 5–7.

Sensory Evaluation of Oral Comfort and Acceptability

Sensory evaluation was conducted to examine how the concentration-dependent mechanical transitions described earlier were perceived during oral manipulation, with emphasis on ease of oral transport, ease of palatal release, and overall acceptability. These sensory attributes were intended to provide supportive perceptual descriptors of oral processing behavior under controlled conditions, rather than to serve as a clinical swallowing assessment.

No statistically significant differences were observed among formulations for any of the evaluated sensory attributes (Fig. 4). Accordingly, the sensory results were interpreted only as supportive perceptual observations and were not used to rank the formulations. Within this scope, the sensory scores generally indicated that the formulations remained within a comparable perceptual range despite substantial differences in instrumental rheological and mechanical properties (Nishinari et al., 2019).

Taken together, these findings suggest that although powder concentration strongly influenced macroscopic deformation behavior, the trained panel did not distinguish the formulations as significantly different in the evaluated sensory dimensions under the present test conditions. Therefore, the sensory results are discussed here as complementary observations that accompany, but do not independently determine, the formulation-level interpretation of structural transition.

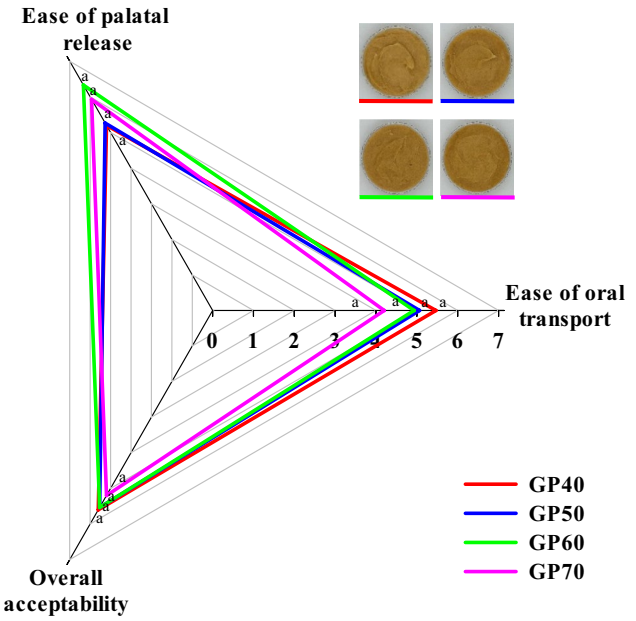


Fig. 4 Sensory scores for ease of oral transport, ease of palatal release, and overall acceptability of ginseng starch pastes. GP40, GP50, GP60, and GP70 denote formulation codes indicating increasing ginseng powder levels across the concentration gradient. Mean values ($n = 30$). No significant differences were observed among samples ($p > 0.05$)

behavior, large-deformation mechanics, and sensory variables exhibited coherent co-variation across the imposed concentration gradient. Pearson correlation, hierarchical clustering, and PCA were used to examine concentration-aligned associations among independently measured variables in the semi-solid matrix (Pan et al., 2021).

Correlation analysis revealed two dominant clusters exhibiting strong antagonistic trends (Fig. 5A). Moisture content, adhesiveness, ease of oral transport, and overall acceptability were strongly positively correlated ($r > 0.70$), representing lubrication-dominated, fluid-like systems typical of GP40–GP50. In contrast, soluble solids, total sugars, saponins, ginsenosides (Rg_1, Rb_1), and antioxidant indices (TPC, DPPH, and ABTS) formed a second cluster negatively associated with the first ($r < -0.60$). This pattern is consistent with concentration-dependent solid-loading behavior in hydrated biopolymer systems, in which increasing solid content is associated with greater compositional density and altered macroscopic structural behavior (Bu et al., 2023; Jiang et al., 2021).

Mechanical parameters, including hardness, gumminess, adhesiveness, cohesiveness, and rupture distance, occupied intermediate positions between the compositional and sensory clusters. This pattern is consistent with a formulation-level association between concentration-dependent structural

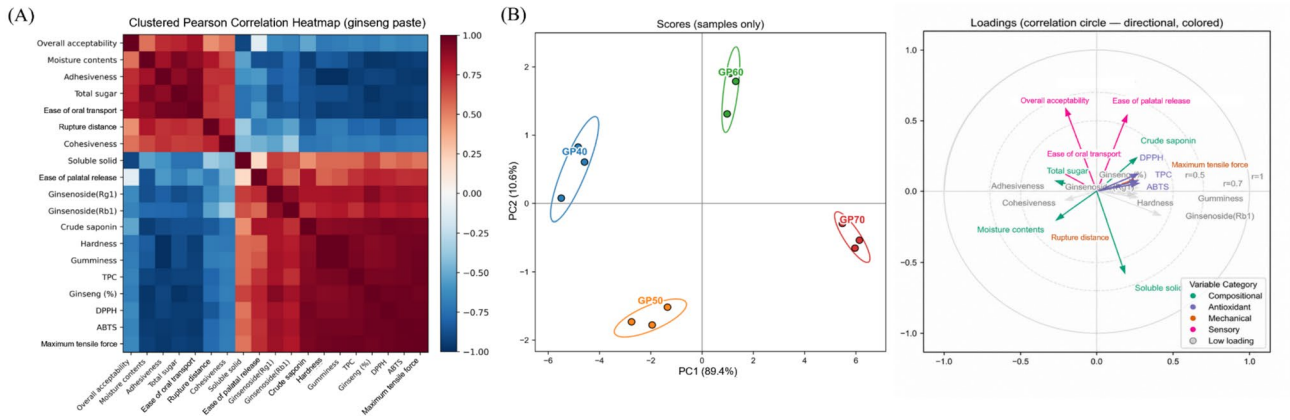


Fig. 5 Integrated multivariate analysis revealing concentration-driven structure–function relationships in ginseng starch pastes. GP40, GP50, GP60, and GP70 denote formulation codes corresponding to increasing ginseng powder levels. Pearson's correlation coefficients (r) are represented by color intensity (red, positive; blue, negative), with values ranging from −1 to +1. Hierarchical clustering was performed using Ward's linkage method with Euclidean distance to identify variable associations. All variables were standardized (z-scored) prior to PCA. PC1 and PC2 explained 89.4% and 10.8% of the total variance, respectively, indicating that concentration-driven variation was the primary source of system differentiation

Integrated Multivariate Interpretation of Concentration-Driven Structure–Function Transitions

Multivariate analyses were conducted to descriptively examine whether physicochemical composition, rheological

reinforcement and perceptual observations, without implying a direct mechanistic linkage. As concentration increased, mechanical resistance also increased, reflecting the progressive reinforcement of the paste matrix under deformation.

PCA further resolved these patterns into a coherent concentration axis (Fig. 5B). PC1 explained 89.4% of the total

variance and represented increasing solid content, with positive loadings for saponins, ginsenosides, antioxidant capacities, and large-deformation resistance. GP40–GP50 mapped to high-moisture, low-rigidity regions characteristic of fluid-dominant pastes, whereas GP60–GP70 were positioned in regions of high compositional density and strong mechanical reinforcement, consistent with soft-solid behavior in concentrated starch matrices (Zhuang et al., 2022). PC2 (10.6%) captured variation related to deformation continuity and cohesive behavior, differentiating GP50 from GP60 within the intermediate concentration range, where several instrumental properties showed transitional behavior. Importantly, this outcome supports that independently acquired variables co-varied consistently with concentration, supporting the internal coherence of the formulation-level structure–function framework rather than implying emergent or independent multivariate relationships. Given the limited number of formulation levels, the multivariate analyses were not intended for statistical inference or model generalization, but rather to visualize concentration-aligned covariation among independently measured properties. Within this context, powder concentration should be interpreted as a formulation-level variable that integrates multiple concentration-dependent changes, rather than as an isolated mechanistic determinant of hydration, gelatinization, or matrix interactions.

Overall, the multivariate results support a coherent formulation-level pattern in which powder concentration is associated with compositional enrichment, mechanical reinforcement, and supportive sensory observations across the concentration gradient. Within the defined scope of this study, powder concentration can be interpreted as a key formulation-level variable linked to nutritional density, macroscopic deformation behavior, and sensory variables, without implying isolation of underlying physicochemical mechanisms.

Conclusions

This study establishes powder concentration as a single, formulation-level control parameter governing the process–structure–function behavior of fresh ginseng starch pastes. Increasing powder concentration was associated with enhanced network densification and a progressive transition from cohesive, flow-dominated pastes to increasingly elastic and shape-retaining soft solids. These structural transitions were reflected consistently across steady-shear flow behavior, viscoelastic spectra, and large-deformation responses, demonstrating that concentration regulates both the energy-storing and dissipative capacities of the system at the macroscopic level. Higher solid content also improved functional retention, with saponins and ginsenosides exhibiting greater stability within denser starch matrices. Mechanical deformation tests and texture profile analysis further indicated that concentration-driven densification increased hardness and adhesiveness while reducing ductility, collectively shaping oral-processing behavior. The combined rheological and IDDSI results indicated that increasing solids loading was associated with a progressive shift from more easily deformable pastes toward more deformation-resistant soft-solid structures across the observed Levels 5–7. Multivariate analysis demonstrated coherent clustering among compositional, rheological, mechanical, and sensory attributes along the concentration gradient. It should be noted that the present work was intentionally framed as a formulation-level investigation rather than a translational or clinical validation study. Because direct water-state measurements such as LF-NMR were not performed, mechanistic interpretation of water redistribution within the matrix remains limited and should be addressed in future work. Accordingly, shelf-life stability during storage, concentration uniformity control under large-scale processing, and cost benchmarking against commercial dysphagia foods were beyond the scope of this study and warrant systematic investigation in subsequent translational research. Within these defined boundaries, the present findings demonstrate that powder concentration alone can function as a simplified and effective design variable for texture-adapted, nutritionally enriched semi-solid foods intended for dysphagia-oriented applications.

Supplementary Information The online version contains supplementary material available at https://doi.org/10.1007/s11947-026-04418-7.

Author Contribution Jiyoon Kim – Conceptualization, Data curation, Formal analysis, Project administration, Investigation, Validation, Visualization, Writing – original draft, Writing – review & editing Jung Soo Kim – Formal analysis, Investigation, Methodology, Validation, Writing – review & editing Kwang-Deog Moon – Funding acquisition, Resources Jung-Ho Lim – Funding acquisition, Resources Jung-Seok Cho – Writing – review & editing, Project administration, Funding acquisition, Supervision.

Funding This work was supported by Basic Science Research Program through the National Research Foundation of Korea (NRF) funded by the Ministry of Education (2022R1A6A3A13065711) and the Korea Institute of Planning and Evaluation for Technology in Food, Agriculture, and Forestry (IPET) through the High Value-Added Food Technology Development Program funded by the Ministry of Agriculture, Food, and Rural Affairs (MAFRA) (321049–5).

Data Availability All data generated or analyzed during this study are included in this article and its supplementary information files. Additional raw datasets are available from the corresponding author upon reasonable request.

Declarations

Competing Interests The authors declare no competing interests.

References

AOAC. (1984). Official methods of analysis of the Association of Official Analytical Chemists (14th ed.). Association of Official Analytical Chemists, Arlington, VA.

Bitencourt, B. S., Guedes, J. S., Saliba, A. S. M. C., Sartori, A. G. O., Torres, L. C. R., Amaral, J. E. P. G., Alencar, S. M., Maniglia, B. C., & Augusto, P. E. D. (2023). Mineral bioaccessibility in 3D printed gels based on milk/starch/κ-carrageenan for dysphagic people. *Food Research International, 170*, Article 113010. https://doi.org/10.1016/J.FOODRES.2023.113010

Brand-Williams, W., Cuvelier, M. E., & Berset, C. (1995). Use of a free radical method to evaluate antioxidant activity. *LWT - Food Science and Technology, 28*(1), 25–30. https://doi.org/10.1016/S0023-6438(95)80008-5

Bu, Q., Chen, Y., Ding, Y., Zhang, K., Li, Y. C., You, X., & Zhao, G. (2023). Preparation and characterization of tea polyphenol composite microspheres encapsulated using sodium alginate and crosslinked starch. *LWT - Food Science and Technology, 184*, Article 114888. https://doi.org/10.1016/J.LWT.2023.114888

Cho, C.-W., Kim, Y.-C., Rhee, Y. K., Lee, Y.-C., Kim, K.-T., & Hong, H.-D. (2014). Chemical composition characteristics of Korean straight ginseng products. *Journal of Ethnic Foods, 1*(1), 24–28. https://doi.org/10.1016/J.JEF.2014.11.007

Costa, M. E., Sarinho, A. M., Lima, J., Andrade, R., Baptista, L., Almeida, R. D., & Lisboa, H. M. (2026). Chemical modification of starch for high-performance bioplastics: A critical review of structure–property relationships and scalable processing. *Carbohydrate Polymers, 378*, Article 124906. https://doi.org/10.1016/j.carbpol.2026.124906

Cui, L., Wang, X., Zhang, J., Ai, Z., Hu, Y., Liu, S., Tang, P., Zou, H., Li, X., Wang, Y., Nan, B., & Wang, Y. (2024). Physicochemical properties and in vitro digestibility of ginseng starches under citric acid-autoclaving treatment. *International Journal of Biological Macromolecules, 265*, Article 131031. https://doi.org/10.1016/J.IJBIOMAC.2024.131031

de Oliveira Zanuso, B., de Oliveira dos Santos, A. R., Miola, V. F. B., Gissoni Campos, L. M., Spilla, C. S. G., & Barbalho, S. M. (2022). *Panax ginseng* and aging related disorders: A systematic review. *Experimental Gerontology, 161*, Article 111731. https://doi.org/10.1016/J.EXGER.2022.111731

Dick, A., Bhandari, B., & Prakash, S. (2021). Printability and textural assessment of modified-texture cooked beef pastes for dysphagia patients. *Future Foods, 3*, Article 100006. https://doi.org/10.1016/J.FUFO.2020.100006

Dubois, M., Gilles, K. A., Hamilton, J. K., Rebers, P. A., & Smith, F. (2002). Colorimetric method for determination of sugars and related substances. *Analytical Chemistry, 28*(3), 350–356. https://doi.org/10.1021/AC60111A017

Fiszman, S., & Laguna, L. (2023). Food design for safer swallowing: Focusing on texture-modified diets and sensory stimulation of swallowing via transient receptor potential activation. *Current Opinion in Food Science, 50*, Article 101000. https://doi.org/10.1016/J.COFS.2023.101000

Gibouin, F., van der Sman, R., Benedito, J., & Della Valle, G. (2022). Rheological properties of artificial boluses of cereal foods enriched with legume proteins. *Food Hydrocolloids, 122*, Article 107096. https://doi.org/10.1016/J.FOODHYD.2021.107096

Guan, T., Ren, C., Feng, Y., Gao, Y., Wang, Q., Rao, S., Xiao, L., Yang, Z., & Liu, Q. (2024). Implementation of succinylated lactoferrin-luteolin nanocomplex-based 3D printing inks in nutritional and textural customization for dysphagia diets: Printing mechanism, improved bioactivity and in vitro bioaccessibility. *LWT - Food Science and Technology, 214*, Article 117115. https://doi.org/10.1016/J.LWT.2024.117115

Hyun, K., Kim, S. H., Ahn, K. H., & Lee, S. J. (2011). A review of nonlinear oscillatory shear tests: Analysis and application of large amplitude oscillatory shear (LAOS). *Progress in Polymer Science, 36*(12), 1697–1753. https://doi.org/10.1016/j.progpolymsci.2011.02.002

International Dysphagia Diet Standardisation Initiative. (2019). Complete IDDSI framework detailed definitions 2.0: 31 July 2019. International Dysphagia Diet Standardisation Initiative. Retrieved from https://www.iddsi.org/

Jiang, G., Feng, X., Wu, Z., Li, S., Bai, X., Zhao, C., & Ameer, K. (2021). Development of wheat bread added with insoluble dietary fiber from ginseng residue and effects on physiochemical properties, in vitro adsorption capacities and starch digestibility. *LWT - Food Science and Technology, 149*, Article 111855. https://doi.org/10.1016/J.LWT.2021.111855

Kim, J., Kim, J. S., Lim, J. H., & Moon, K. D. (2024a). Effects of isolated pea protein on honeyed red ginseng manufactured by 3D printing for patients with dysphagia. *LWT - Food Science and Technology, 191*, Article 115570. https://doi.org/10.1016/J.LWT.2023.115570

Kim, J., Kim, J. S., & Moon, K. D. (2025). 3D-printed rice cake for dysphagia diet: Effect of rice flour/κ-carrageenan/curdlan complex gel on structure, swallowability, and storage. *Future Foods, 11*, Article 100537. https://doi.org/10.1016/J.FUFO.2024.100537

Kim, J. S., Kim, J., Nam, I., Kim, S. H., Seo, Y. M., Lim, J. H., & Moon, K. D. (2024). Effect of red ginseng extract on the quality characteristics of mayonnaise. *Food Science and Preservation, 31*(5), 800–810. https://doi.org/10.11002/FSP.2024.31.5.800

Koo, H. J., Park, S. H., Jo, J. S., Kim, B. Y., & Baik, M. Y. (2005a). Gelatinization and retrogradation of 6-year-old Korean ginseng starches studied by DSC. *LWT - Food Science and Technology, 38*(1), 59–65. https://doi.org/10.1016/J.LWT.2004.05.003

Koo, H. J., Park, S. H., Jo, J. S., Kim, B. Y., Hur, N. Y., & Baik, M. Y. (2005b). Physicochemical characteristics of 6-year-old Korean ginseng starches. *LWT - Food Science and Technology, 38*(8), 801–807. https://doi.org/10.1016/J.LWT.2004.10.009

Lee, H., Kim, Y.-S., Kim, D.-Y., Kim, S.-Y., Lee, W.-K., Lee, S.-M., Park, J.-D., & Shon, M.-Y. (2015). A study on manufacturing of red ginseng Makgeolli using the red ginseng starch and changes of physicochemical components of red ginseng Makgeolli during storage periods. *Food Science and Preservation, 22*(3), 369–376. https://doi.org/10.11002/KJFP.2015.22.3.369

Lee, S. W., & Rhee, C. (2007). Effect of heating condition and starch concentration on the structure and properties of freeze-dried rice starch paste. *Food Research International, 40*(2), 215–223. https://doi.org/10.1016/J.FOODRES.2006.05.005

Li, R., Ding, L., Guo, K., Qu, J., Herburger, K., Persson, S., Blennow, A., & Zhong, Y. (2023). The effects of different types of high-amylose maize starches on viscosity and digestion of acidified milk gels. *Food Chemistry, 404*, Article 134525. https://doi.org/10.1016/J.FOODCHEM.2022.134525

Liu, B., Zhong, F., Yokoyama, W., Huang, D., Zhu, S., & Li, Y. (2020). Interactions in starch co-gelatinized with phenolic compound systems: Effect of complexity of phenolic compounds and amylose content of starch. *Carbohydrate Polymers, 247*, Article 116667. https://doi.org/10.1016/J.CARBPOL.2020.116667

Liu, Z., Chen, X., Dai, Q., Xu, D., Hu, L., Li, H., Hati, S., Chitrakar, B., Yao, L., & Mo, H. (2023). Pea protein-xanthan gum interaction driving the development of 3D printed dysphagia diet. *Food Hydrocolloids, 139*, Article 108497. https://doi.org/10.1016/J.FOODHYD.2023.108497

Merino, G., Gómez, I., Marín-Arroyo, M. R., Beriain, M. J., & Ibañez, F. C. (2020). Methodology for design of suitable dishes for dysphagic people. *Innovative Food Science & Emerging Technologies, 64*, Article 102383. https://doi.org/10.1016/J.IFSET.2020.102383

Methacanon, P., Kongjaroen, A., & Gamonpilas, C. (2023). Structural and shear and extensional rheological properties of hairy basil seed mucilage for potential application as oropharyngeal dysphagia diets. *Food Hydrocolloids, 143*, Article 108903. https://doi.org/10.1016/J.FOODHYD.2023.108903

Mursaliyeva, V. K., Sarsenbek, B. T., Dzhakibaeva, G. T., Mukhanov, T. M., & Mammadov, R. (2023). Total content of saponins, phenols and flavonoids and antioxidant and antimicrobial activity of in vitro culture of *Allochrusa gypsophiloides* (Regel) Schischk compared to wild plants. *Plants, 12*(20), Article 3521. https://doi.org/10.3390/PLANTS12203521

Nishinari, K., Turcanu, M., Nakauma, M., & Fang, Y. (2019). Role of fluid cohesiveness in safe swallowing. *Npj Science of Food, 3*(1), 1–13. https://doi.org/10.1038/S41538-019-0038-8

Oberoi, D. P. S., & Sogi, D. S. (2015). Effect of drying methods and maltodextrin concentration on pigment content of watermelon juice powder. *Journal of Food Engineering, 165*, 172–178. https://doi.org/10.1016/J.JFOODENG.2015.06.024

Pan, Y., Sun, Q., Liu, Y., Wei, S., Xia, Q., Zheng, O., Liu, S., Ji, H., Deng, C., & Hao, J. (2021). The relationship between rheological and textural properties of shrimp surimi adding starch and 3D printability based on principal component analysis. *Food Science & Nutrition, 9*(6), 2985–2999. https://doi.org/10.1002/FSN3.2257

Rahman, M. S., & Al-Farsi, S. A. (2005). Instrumental texture profile analysis (TPA) of date flesh as a function of moisture content. *Journal of Food Engineering, 66*(4), 505–511. https://doi.org/10.1016/J.JFOODENG.2004.04.022

Ren, R., Pellegrini, N., Proteggente, A., Pannala, A., Yang, M., & Rice-Evans, C. (1999). Antioxidant activity applying an improved ABTS radical cation decolorization assay. *Free Radical Biology & Medicine, 26*(9–10), 1231–1237. https://doi.org/10.1016/S0891-5849(98)00315-3

Sharma, K., Kaur, R., Kumar, S., Saini, R. K., Sharma, S., Pawde, S. V., & Kumar, V. (2023). Saponins: A concise review on food related aspects, applications and health implications. *Food Chemistry Advances, 2*, Article 100191. https://doi.org/10.1016/J.FOCHA.2023.100191

Singh, S., & Kaur, M. (2017). Steady and dynamic shear rheology of starches from different oat cultivars in relation to their physicochemical and structural properties. *International Journal of Food Properties, 20*(12), 3282–3294. https://doi.org/10.1080/10942912.2017.1286504

Stading, M. (2021). Bolus rheology of texture-modified food: Effect of degree of modification. *Journal of Texture Studies, 52*(5–6), 540–551. https://doi.org/10.1111/JTXS.12598

Steele, C. M., Alsanei, W. A., Ayanikalath, S., Barbon, C. E. A., Chen, J., Cichero, J. A. Y., Coutts, K., Dantas, R. O., Duivestein, J., Giosa, L., Hanson, B., Lam, P., Lecko, C., Leigh, C., Nagy, A., Namasivayam, A. M., Nascimento, W. V., Odendaal, I., Smith, C. H., & Wang, H. (2015). The influence of food texture and liquid consistency modification on swallowing physiology and function: A systematic review. *Dysphagia, 30*(1), 2–26. https://doi.org/10.1007/S00455-014-9578-X

Witt, T., & Stokes, J. R. (2015). Physics of food structure breakdown and bolus formation during oral processing of hard and soft solids. *Current Opinion in Food Science, 3*, 110–117. https://doi.org/10.1016/J.COFS.2015.06.011

Xiang, Y., Zou, M., Ou, F., Zhu, L., Xu, Y., Zhou, Q., & Lei, C. (2024). A comparison of the impacts of different drying methods on the volatile organic compounds in ginseng. *Molecules, 29*(22), Article 5235. https://doi.org/10.3390/MOLECULES29225235

Yu, X., Wang, Y., Zhao, W., Li, S., Pan, J., Prakash, S., & Dong, X. (2023). Hydrophilic colloids (konjac gum/xanthan gum) in 3D printing of transitional food from fish paste. *Food Hydrocolloids, 137*, Article 108333. https://doi.org/10.1016/J.FOODHYD.2022.108333

Zhao, B., Lv, C., & Lu, J. (2019). Natural occurring polysaccharides from *Panax ginseng* C. A. Meyer: A review of isolation, structures, and bioactivities. *International Journal of Biological Macromolecules, 133*, 324–336. https://doi.org/10.1016/J.IJBIOMAC.2019.03.229

Zhuang, H., Li, X., Wu, S., Zhao, J., Gao, Y., & Yan, H. (2022). Application of ginseng powder and combined starter culture for improving the oxidative stability, microbial safety and quality characteristics of sausages. *LWT - Food Science and Technology, 166*, Article 113749. https://doi.org/10.1016/J.LWT.2022.113749

Publisher's Note Springer Nature remains neutral with regard to jurisdictional claims in published maps and institutional affiliations.

Springer Nature or its licensor (e.g. a society or other partner) holds exclusive rights to this article under a publishing agreement with the author(s) or other rightsholder(s); author self-archiving of the accepted manuscript version of this article is solely governed by the terms of such publishing agreement and applicable law.